STUDIES OF IMPEDANCE IN CARDIAC TISSUE USING SUCROSE GAP AND COMPUTER TECHNIQUES

II. Circuit Simulation of Passive Electrical Properties and Cell-to-Cell Transmission

GEORGE R. STIBITZ and FRANCES V. McCANN

From the Department of Physiology, Dartmouth Medical School, Hanover, New Hampshire 03755

ABSTRACT The impedance measured in a strip of heart tissue from the moth *Hyalophora cecropia* is fitted by circuit models of several configurations. The circuits include: (*a*) a single R-C circuit (*b*) a double R-C circuit (*c*) terminated transmission lines, and (*d*) a pattern of cells with cell-to-cell transmission paths. The last of these is found to give the best fit. Calculation of the model impedances and optimization of element values are performed by a computer. The possibility that the mechanism of cell-to-cell transmission may be capacitative rather than conductive is explored using values of capacitance derived from the circuit models to calculate the effect of capacitative coupling alone on signal transmission. The calculations show that sufficient voltage can be transmitted from the excited cell to an adjacent cell to effect excitation.

A. EQUIVALENT CIRCUIT MODELS

A pervasive model circuit depicts the passive electrical properties of excitable tissues and particularly of nerve by representing the cell membrane as a simple R-C circuit consisting of a single capacitor connected in parallel with a resistive element. This simple scheme does not now appear applicable to muscle cells and more particularly to cardiac cells. An electrical network with at least two "time constants," probably due to multiple infoldings of the membrane and to the indentations of the transverse tubules, has been proposed to represent Purkinje fibers (Fozzard, 1966; Freygang and Trautwein, 1970). This topic is reviewed and summarized by Fozzard (1972).

This paper considers circuit models which simulate impedances measured in the heart of the adult moth, *H. cecropia* by a gap technique. The measurements were reported in the first paper of this series (McCann et al., 1973). While it has been

noted that the numerical values of impedance obtained in the sucrose gap change with time, and must, therefore, be accepted with certain reservations, still the general form of the impedance function does not change with time, and therefore appears reliable. Since the configuration of the model circuit is primarily determined by the shape of the impedance function, we believe that the conclusions reached regarding the configurations of the models presented here are valid.

In this study, configurations or arrangements of resistive and capacitative elements have been chosen empirically with regard to the physical structure of the tissue being represented. The computing facilities of the Dartmouth time-share computing center have been employed extensively, and programs have been written which embody the circuit equations of the models. The program, described in the Appendix, instructs the computer to optimize the parameter values for the "best" fit between the model and the experimental impedances. The criterion used here for the best fit is the minimum value of a weighted sum of squares of the differences in modulus and angle between the two impedances.

Measurement and fitting of models have been based on impedances rather than on indicial admittance functions (step functions). While the theory of communications systems shows that both representations are equally valid, the equality assumes that no noise is present, and that the measuring equipment used is capable of recording accurately within a negligible time period. Impedance measurements are made in very narrow frequency bands and the noise in such bands is relatively unimportant. Furthermore, analysis of time functions is difficult and sensitive to errors.

All models treated here assume the measured tissue to be a cylindrical body surrounded by three pools of fluid, of which the center pool is an insulating medium. The end pools contain electrolytes in which electrodes are immersed to serve as electrical connections to an impedance bridge (Stibitz et al., 1973).

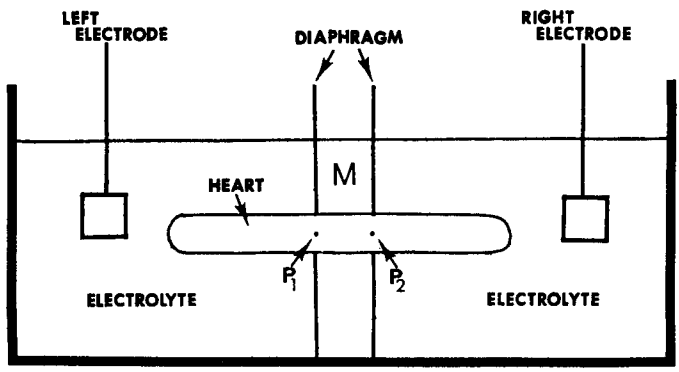

FIGURE 1 A schematic diagram of the tissue specimen in the sucrose gap. The heart is cylindrical and passes through holes in rubber diaphragms which separate the right and left electrolyte pools from the central insulating medium, M. Impedance is measured between the left and right electrodes. Points P_1 and P_2 (see text) lie on the axis of the cylinder and in the planes of the diaphragms.

Fig. 1 is a schematic of the experimental setup. The total impedance between the electrodes in the end pools is the sum of Z_1 impedance between the left electrode and point P_1, Z_2 impedance between points P_1 and P_2 and Z_3, impedance between P_2 and the right electrode. It is assumed that the currents induced by the bridge flow longidinally in the portion of the specimen immersed in the insulating fluid, and that these currents flow from the electrodes, by way of the electrolyte, through the cell membranes and into the myoplasm of cells or portions of cells immersed in the electrolyte pools.

The total impedance between the electrodes has been found for a large number of specimens and data from one experiment have been selected for the modeling operation. Fig. 2 is a reproduction of a computer plot showing the impedance both as a curve in the complex plane and as modulus and angle functions of frequency.

The simple R-C model previously referred to is seen in Fig. 3. At a frequency of $\omega/2\pi$ the model impedance has the form

$$Z = Z_1 + Z_2 + Z_3,$$

where

$$1/Z_1 = i\omega C_1 + 1/R_1$$

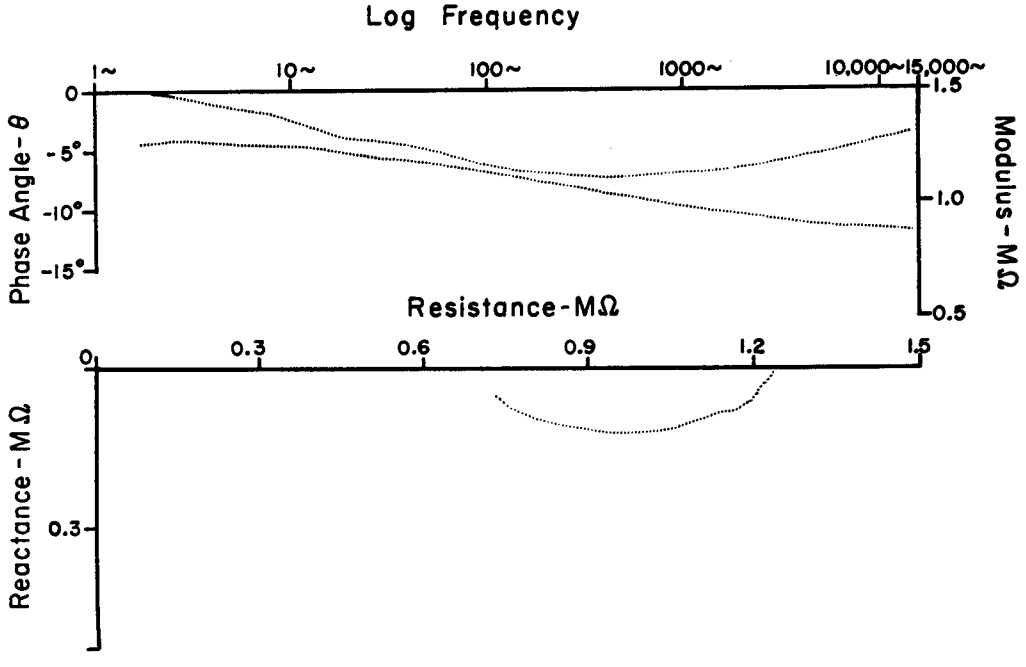

FIGURE 2 Plots of the measured impedance of a specimen arranged as in Fig. 1. The lowest curve shows the impedance plotted on the complex plane. The upper curves are, respectively, the angle and the modulus of the impedance plotted as functions of frequency.

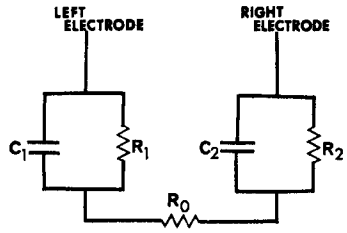

FIGURE 3 Circuit schematic for a simple model of the specimen of Fig. 1. C_1 and C_2 represent the capacitances of the portions of the membrane in the left and right electrolyte pools, respectively. R_1 and R_2 are the corresponding leakage resistances. R_0 is the longitudinal resistance of the portion of the specimen in the insulating pool.

$$Z_2 = R_0$$

$$1/Z_3 = i\omega C_2 + 1/R_2.$$

If the membrane is homogeneous, then $R_1 C_1 = R_2 C_2$ and Z becomes the impedance of a single capacitor, $C_1 C_2/(C_1 + C_2)$, in parallel with a resistance $R_1 + R_2$. The computer program previously mentioned has optimized the values of resistance and capacitance and found $R_0 = 0.3397\ \Omega$, $C_1 = 0.00118$ mF, $R_1 = 0.7959$ mΩ, $E = 0.974$ arbitrary units, where E is a measure of the discrepancy between the simulated and measured impedances. Further details of this measure are presented in the Appendix.

Comparison of the model impedance (solid lines) with the measured impedance (dotted lines) in Fig. 4 shows that the model is completely inadequate for the cell of the moth heart. Furthermore, it is well known that any circuit which contains a single capacitor and any number of resistors has an impedance which, like that plotted in Fig. 4, is a semicircle on the complex plane, and would be equally unsatisfactory.

We conclude that the specimen under investigation does not have a single "time constant," that it cannot be modeled with a single capacitor, and that its response to a step function, while qualitatively similar to an exponential in time, cannot be so represented.

The model may be elaborated according to the suggestion (Fozzard, 1972) that the sarcolemmal invaginations or transverse tubular system observed in many excitable cells may account for a second capacitance, and hence for a noncircular impedance plot. The second capacitance would be in electrical connection with the electrolyte by way of high resistance paths along the tubules. This suggestion leads to the model presented in Fig. 5 A.

The circuit of Fig. 5 A is not minimal, in the sense that there exists another circuit with fewer elements but identical impedance. Fig. 5 B shows a circuit which is

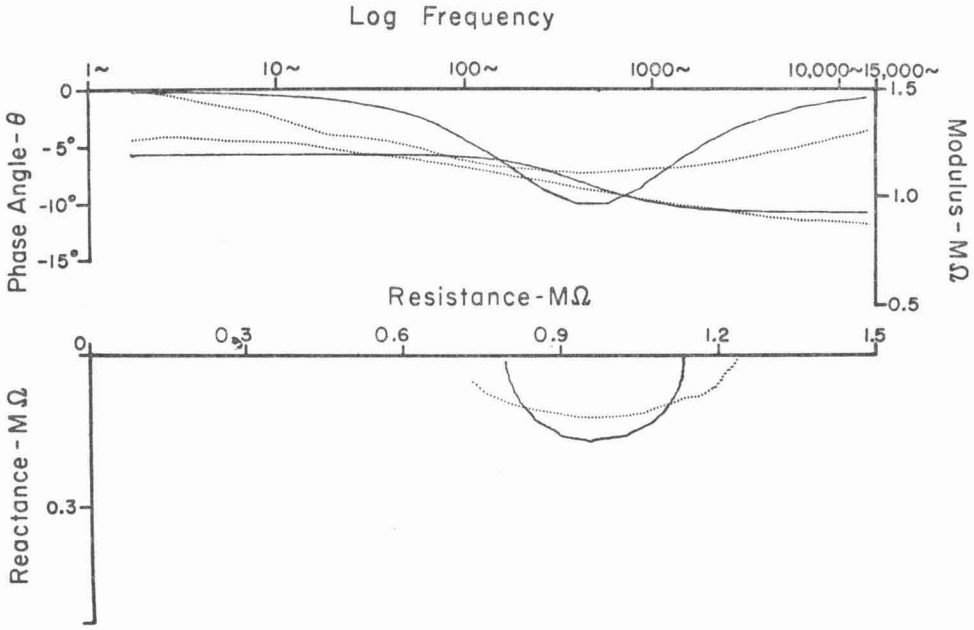

FIGURE 4 Impedance plots comparing the electrical properties measured in the specimen with that of the simple model of Fig. 3. The impedance of the specimen, shown by dotted curves, is superimposed on that of the model. Both are plotted according to the plan of Fig. 2.

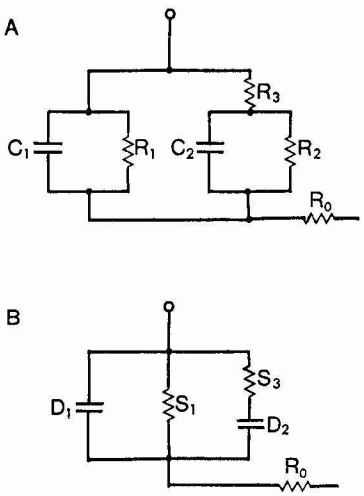

FIGURE 5 (*A*) Schematic of a model that includes the transverse-tubule system. C_1, R_1, represent the capacitance and leakage, respectively, of the cell membrane. C_2 and R_2 represent capacitance and resistance, respectively, of the transverse tubules. R_3 represents the longitudinal resistance of the medium within the tubules. (*B*) Schematic of a circuit with a minimal number of elements, equivalent at all frequencies to that of Fig. 5 *A*.

electrically equivalent to that of Fig. 5 A if

$$D_1 = C_1 \qquad S_1 = R_1 (R_2 + R_3)/(R_1 + R_2 + R_3)$$

$$D_2 = R_2^2/(R_2 + R_3)^2 C_2 \qquad S_3 = R_3 (R_2 + R_3)/R_2$$

$$R_0 = R_0$$

The computer program has optimized the values of Fig. 5 B with respect to the measured impedance and found (Fig. 6) $D_1 = 4.117\ 10^{-4}\ \mu F$, $S_1 = 0.4475\ M\Omega$, $D_2 = 1.704\ 10^{-3}\ \mu F$, $S_3 = 0.4378\ M\Omega$, $R_0 = 0.7359\ M\Omega$, $E = 0.155$ arbitrary units.

It will be noted that the agreement between model and experiment is much closer than in the previous simple model, as indicated by the smaller value of E as well as by the appearance of the impedance plots. If the model is to be related to the physical specimen, a decision must now be made as to which of the infinite family of equivalent circuits of Fig. 5 A will be selected. The choice may be made to depend upon one element, say R_2, which may be allowed to vary while the other elements are adjusted accordingly without change in the impedance. A computer program has plotted in arbitrary units the values of R_1, C_2, R_3, corresponding to any value of R_2 from 0.2 to 4.4 MΩ, and infinity (Fig. 7).

It will be noted that C_2 of Fig. 5 B which represents the capacitance of the transverse tubular system, must have a value at least as great as that when R_2 is infinite, or

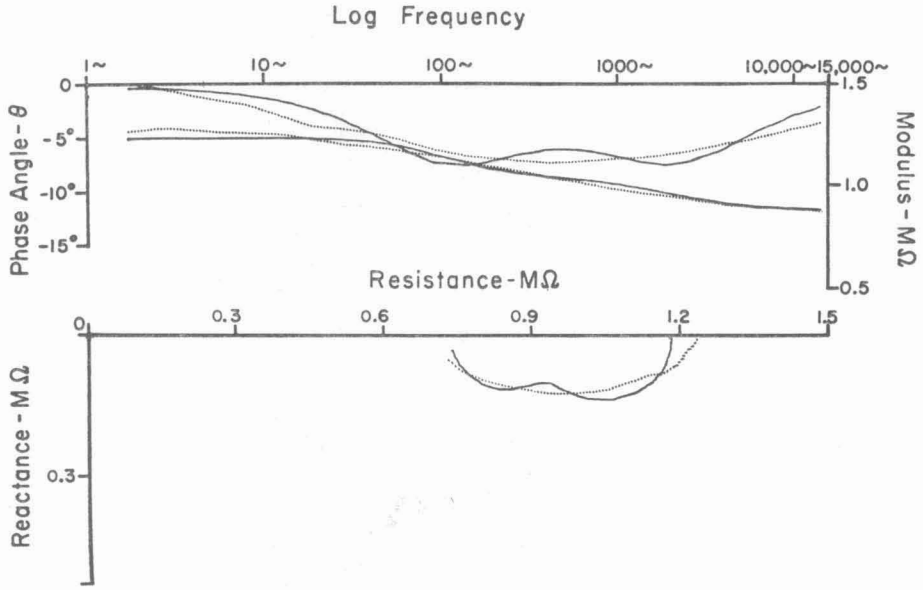

FIGURE 6 Plot of impedances measured on the specimen (dotted line) and of the model depicted in Fig. 5 *B* (solid line).

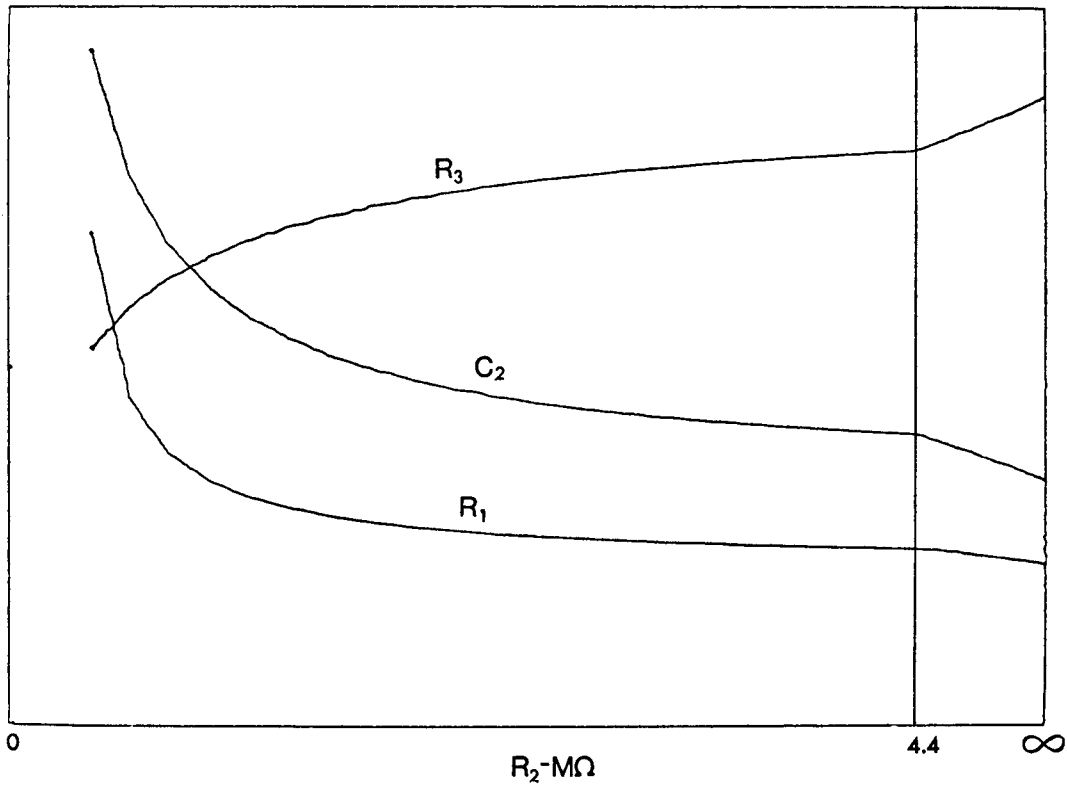

FIGURE 7 Graphs of elements R_1, C_2, R_3 for values of R_2 taken from Fig. 5 *A*. The impedances of any two circuits, formed by inserting into Fig. 5 *A* sets of values chosen in accordance with these graphs, are identical for all frequencies.

$C_2 > 1.704\ 10^{-3}\ \mu F$. This is approximately four times as great as D_1, the membrane capacitance.

Bassingthwaighte and Reuter (1972) deduce a total area of the transverse tubular system approximately equal to that of the total membrane in rat heart cells. Hence, to account for the 4:1 capacitance ratio we need only assume that the tubular boundary is less than ¼ as thick as the membrane, assuming similar physical characteristics. Impedance measurements alone can give us no further information about this model. The two models investigated so far have assumed "lumped" elements and have ignored the obvious fact that the membrane is distributed in space.

Retaining the assumption that the radial dimensions of the specimen are electrically short, we now introduce the concept of a finite transmission line. For the next model we represent that portion of the specimen which lies in the electrolyte by a transmission line in which the membrane is a leaky shunt capacitance. The theory of transmission lines has been treated by Kelvin (1854) for the capacitative cable, and more generally by Heaviside (1887). Heaviside showed that if z_1 is the longitudinal

impedance per unit length of cable and $1/z_2$ is the shunt admittance per unit length, then the impedance seen at one end of the cable is

$$Z = Z_o (1 + T^2)/(1 - T^2)$$

where

$$Z_o = \sqrt{Z_1 Z_2}$$

$$T = \exp (- \sqrt{Z_1/Z_2}\, L).$$

Unlike the lumped-element model, the terminated line model requires us to treat individually the portions of the specimen which lie in the electrolyte pools. However, in the present model we assume that the interior of the cylinder is homogeneous throughout its length, and is resistive.

The formulas for the finite lines, the lengths of the gap and of the two end portions of the specimen have been written into a computer program which calculates the impedance of the specimen for arbitrarily assigned values of the axial resistivity, the leakage, and the capacitance per unit length. Fig. 8 shows the optimized impedance for a gap length of 0.47 cm, a left portion of 0.172 cm and a right portion of 0.328 cm length. The optimum values found are: capacitance, 0.0384 μF/cm; leakage, 0.0264 MΩ·cm; longitudinal resistance, 1.55 MΩ/cm; $E = 0.319$.

Clearly the assumptions underlying this model are not adequate. While better than the corresponding lumped model, the agreement is less satisfactory than for the

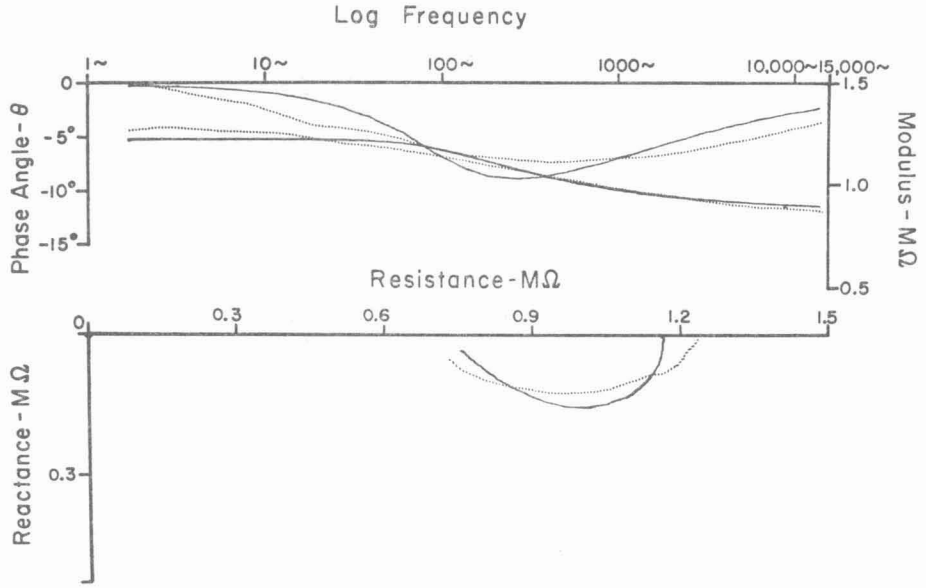

FIGURE 8 The impedance of a model in which finite transmission lines represent the portions of the specimen in the electrolyte pools.

"transverse tubule" model. Our next step recognizes that the medium within the cylinder which represents the specimen is, in the moth heart, not a single cell, but a bundle of small cells, none of which extend from pool to pool. The path followed by currents in the interior of the cylinder is now visualized as a zigzag one, passing from cell to cell in both lateral and longitudinal directions at specialized areas.

Electron microscopic inspection of the specimen (Fig. 9) shows that the cells are not arranged in a regular pattern, but generally appear in columns of end-to-end cells, with appreciable overlap between cells in adjacent columns. For simplicity, however, our model assumes a regular pattern of cells with alternate columns of cells overlapping by half their length (Fig. 10 A).

In this model it is assumed that adjoining cells are coupled electrically through contiguous regions of their membranes, both end-to-end and laterally. The junctions are assigned impedances appropriate to leaky capacitances, and the intracellular region is considered a purely resistive medium. The lateral junctions midway along the overlapping regions between cells are assigned impedance Z_b. The end-to-end junctions have impedance Z_c, while Z_a is the longitudinal impedance between the junction points, or $2Z_a$ is the impedance between the ends of a cell. The cell matrix then is electrically equivalent to the simplified schematic of Fig. 10 B, with the impedances Z_a, Z_d $(= Z_a + Z_c)$ and Z_b. The pattern of impedances is repeated with alternate rectangles inverted as shown. The branch currents are indicated in the figure.

Since we are concerned with longitudinal transmission of currents in the network, we assume zero net transverse current, and find that $I_3 + I_4 = 0$. The longitudinal currents in alternate branches are I_1 and I_2, so that the current per parallel rectangle is $(I_1 + I_2)/2$. If V is the voltage between the end junctions of a cell, we obtain

$$\begin{aligned} V &= I_1 Z_a/2 + I_2 Z_d + I_1 Z_a/2 \\ &= I_1 Z_a + I_2 Z_d. \end{aligned}$$

Tracing the mesh voltage around a rectangle we have

$$\begin{aligned} O &= Z_d I_2 + Z_b I_4 - Z_a I_1 - Z_b I_3 \\ &= Z_d I_2 - Z_a I_1 + 2 Z_b I_4, \end{aligned}$$

since $I_3 + I_4 = 0$. For each node the net current is zero and $0 = I_1 + 2 I_4 - I_2$.

Solving these equations we find the impedance of each cell to be the ratio of V, the voltage between the cell ends to I, the current per cell

$$Z = V/I = 2 \frac{Z_a Z_b + 2Z_a Z_d + Z_b Z_d}{Z_a + 2Z_b + Z_d}.$$

Letting N be the number of parallel columns of cells side-by-side in the specimen,

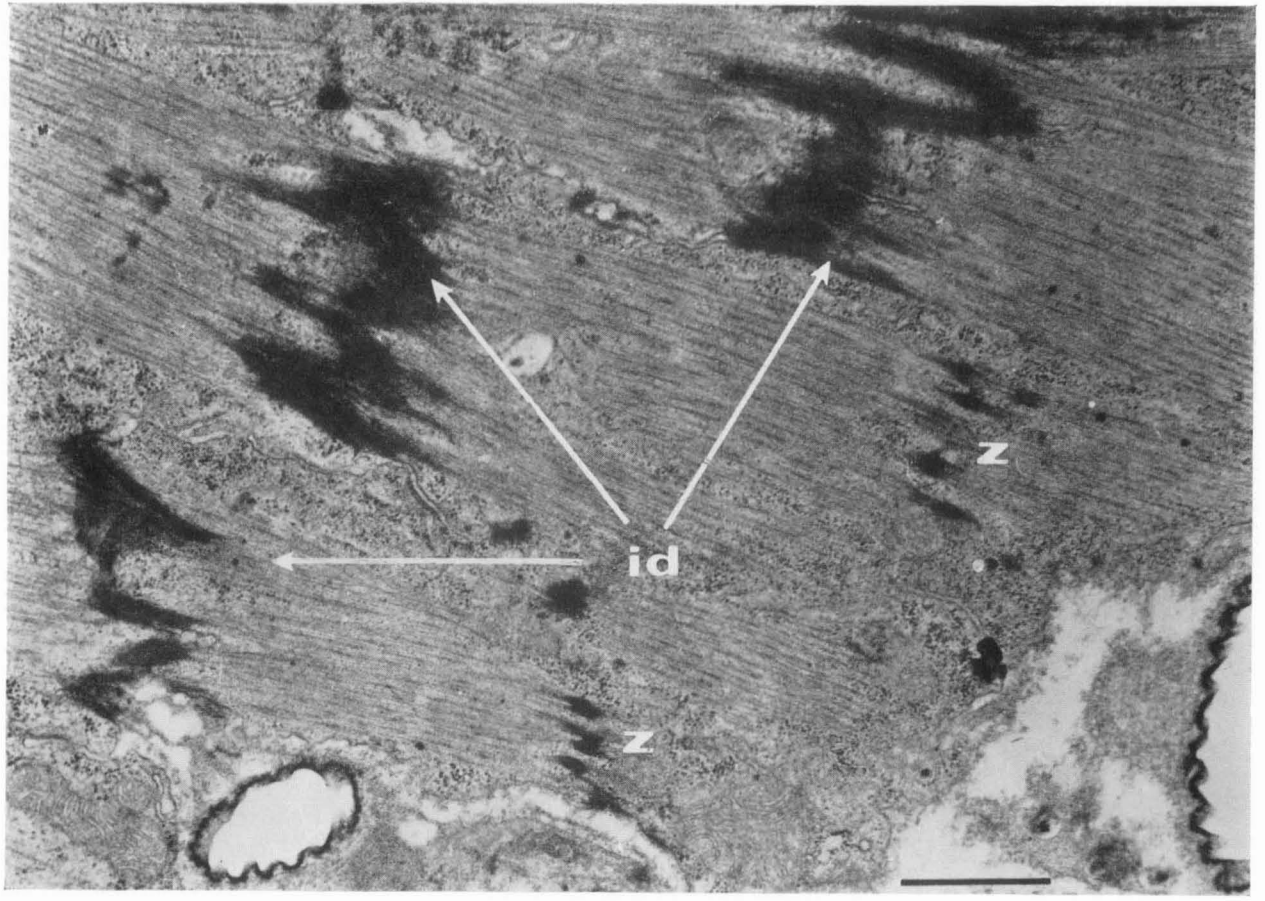

FIGURE 9 An electronmicrograph of a longitudinal section of the *cecropia* heart wall. Intercalated discs are indicated by arrows and letters *id*. Myofilaments are aligned into sarcomere units by transverse dark bodies (*Z*-bands). Marker indicates 1 μm (Sanger, 1967).

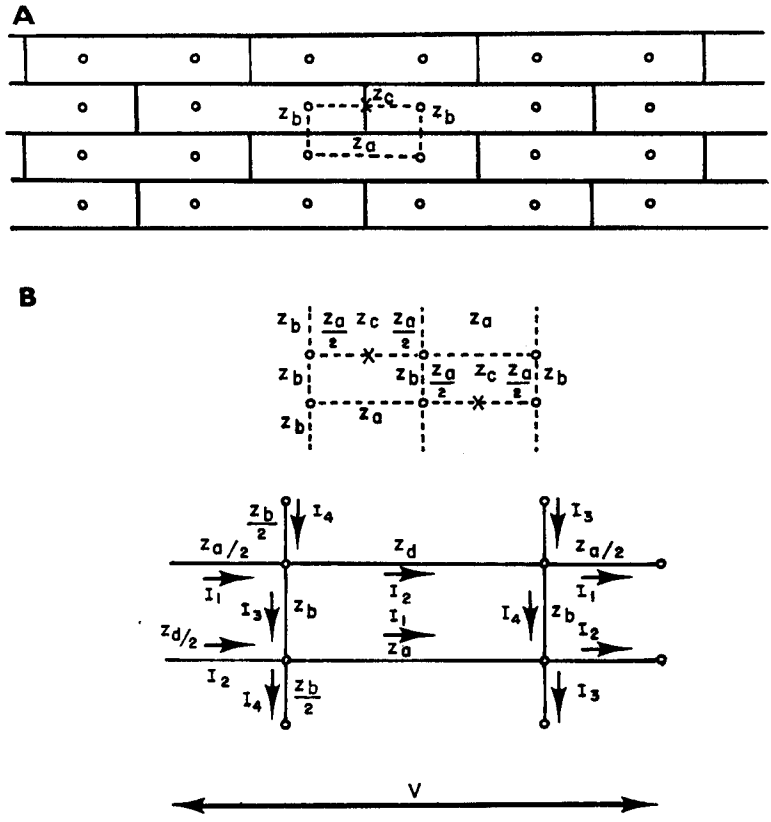

FIGURE 10 (*A*) The geometric arrangement of cells which is assumed in a model for longitudinal transmission through the cylinder of Fig. 1. The impedances within and between cells are indicated as Z_a, Z_b, Z_c. (*B*) A schematic of the circuit implied by the arrangement of cells shown in Fig. 10 *A*. Arrow indicates ends of a single cell at which voltage (V) is measured.

and L the length of a cell, the impedance of a centimeter length of the specimen is $Z_1 = Z/(NL)$.

Since little is known about the electrical properties of the tight junctions in either the lateral or longitudinal connections, and since they have similar microscopic appearance, we feel justified in assuming that their impedances are proportional. Thus, we let $Z_c = K Z_b$ where K is a real number independent of frequency.

In optimizing the parameters of this model, we note that the values of N and L have no essential effect on the impedances, and can be absorbed by renaming the latter. For this model the interior of the cylinder is replaced by the bundle of cells just discussed and the portions of the specimen in the electrolyte pools are leaky capacitances C_1, R_1 in the membrane itself,

$$2\,Z_b/NL = R_2 + 1/(i\omega\,C_2)$$
$$2\,Z_a/NL = R_3.$$

The optimization program finds the plot of Fig. 11, with the impedance values: $C_1 = 0.0227\ \mu F/cm$; $C_2 = 0.0122\ \mu F\text{-cm}$, $R_1 = 1.719\ M\Omega\text{-cm}$, $R_2 = 0.381\ M\Omega/cm$, $R_3 = 0.735\ M\Omega/cm$, $K = 1.06$, $E = 0.044$.

Comparison of the measured and calculated impedances in Fig. 11 shows fair agreement. The model impedance exhibits somewhat more definite bimodality than does the specimen, but it will be recalled that we have assumed exact equality among the cells and perfectly regular arrangement in the meshes. The introduction of random variation would doubtless reduce the clear-cut double hump in the model impedance.

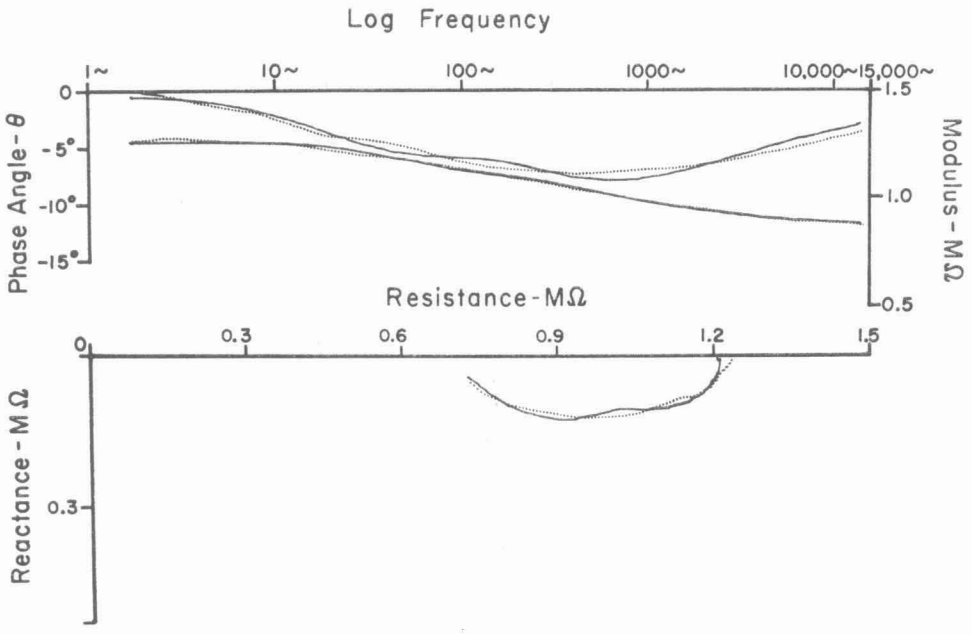

FIGURE 11 The impedance of the model sketched in Fig. 10 (solid line), compared with the measured impedance of specimen (dotted line).

B. A STATISTICAL MODEL OF MEMBRANE IMPEDANCE

One of the classical models designed to represent the passive electrical properties of an excitable cell membrane consists of a capacitance shunted by a conductance, each proportional to the membrane area (Fozzard, 1966; Freygang and Trautwein, 1970; Eisenberg, 1967; McCann et al., 1973). A comprehensive review of this topic has also been published (Cole, 1968). A similar model can be used to represent the passive electrical properties of the interface between an electrode and an electrolyte. A typical plot for the impedance of an electrode-electrolyte interface is shown in Fig. 12.

This model is not entirely satisfactory for either physical system, for it is well

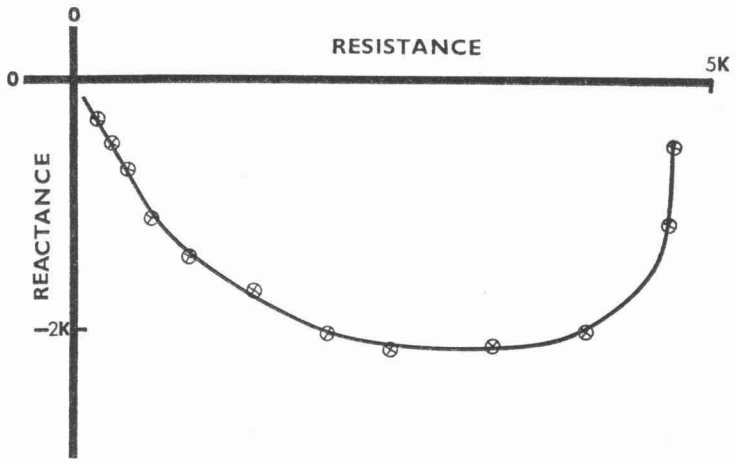

FIGURE 12 Impedance measured at the interface between gold electrodes and physiological (moth) saline. If the interface were represented by a uniform capacitance and leakage, with or without a series resistance, the impedance plot would be a semicircle with its center on the real axis, and at the high-frequency end (left, in the figure) the impedance curve would meet the real axis at right angles.

known that the plot of the impedance of any circuit which contains a single capacitance and any number of resistors is a semicircle. However, plots of the measured impedances of membranes and of electrode interfaces depart considerably from this form. The proportionality of capacitance and conductance to area implies a uniform distribution of the parameters over the membrane or interface. We suggest that only the averages of these quantities over relatively large areas are uniform, and that the capacitance and conductance may vary from point to point in a statistical manner. This study considers the effect on the overall impedance when such point-to-point variations occur.

Each small elementary area of the membrane or electrode interface is represented by either of the equivalent circuits of Fig. 13.

These two circuits are exactly equivalent under all external measurements, provided that

$$R = r\,(1 + rg)$$

$$G = g/(1 + rg)$$

$$C = c/(1 + rg)^2.$$

If one of these circuits represents a small area, S, and the parameters R, C, G are values for a unit area, then for area S we replace C by CS, G by GS, and R by R/S. If A is the specific admittance, then the admittance of the circuit representing area S is

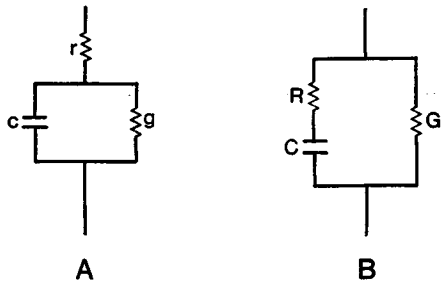

FIGURE 13 Equivalent circuits for infinitesimal element. Circuit A is a model of an infinitesimal region of a cell membrane or of the interface between an electrode and an electrolyte. Conductance, g, represents electrical leakage through the membrane or interface, and resistance, r, represents the resistance of electrolyte in contact with the infinitesimal area. Circuit B is electrically equivalent to A when the element values, C, R, G, are appropriately related to c, r, g (see text).

$$AS = GS + i\omega CS/(1 + i\omega RC),$$

where $\omega = 2\pi$ times the frequency at which the admittance is evaluated.

It will be convenient to write $RC = T$, the "time constant" for the elementary circuit. We may now express the admittance of any small area, S, as $A(G, C, T,)S$. The admittance of a membrane of unit area, is then the sum of the admittances of all such elementary areas, S, since these areas are electrically in parallel.

Let $P(G,C,T)$ be the probability distribution of the parameters, G, C, T, so that the portion of the unit area which has conductance in the range G to $G + \mathrm{d}G$, capacitance C to $C + \mathrm{d}C$, and time constant T to $T + \mathrm{d}T$, is $P(G,C,T)\,\mathrm{d}G\,\mathrm{d}C\,\mathrm{d}T$. The total admittance of all the areas which have these values is

$$P(G,C,T)\,A(G,C,T)\,\mathrm{d}G\,\mathrm{d}C\,\mathrm{d}T.$$

The admittance of the entire unit area at frequency ω then is the sum of all such admittances, or

$$\bar{A} = \iiint P(G, C, T)A(G, C, T)\,\mathrm{d}G\,\mathrm{d}C\,\mathrm{d}T$$

$$= \iiint P(G, C, T)G\,\mathrm{d}G\,\mathrm{d}C\,\mathrm{d}T$$

$$+ \iiint i\omega C/(1 + i\omega T)P(G, C, T)\,\mathrm{d}G\,\mathrm{d}C\,\mathrm{d}T.$$

The first of these two integrals of this last expression merely defines the mean value of G over the surface, and may be called $\bar{G}$. The second may be simplified by introducing the quantity

$$Q(T) = \iint CP(G, C, T)\,\mathrm{d}G\,\mathrm{d}C,$$

which is the mean value of C for all elementary areas having a time constant, T. Then

$$\bar{A} = \bar{G} + i\omega \int Q(T)/(1 + i\omega T)\, dT.$$

The admittance, $\bar{A}$, may be expressed in real and imaginary parts, $\bar{A} = A_1 + i A_2$, by writing

$$A_1 = \bar{G} + \omega^2 \int \frac{Q(T)T\, dT}{1 + \omega^2 T^2}$$

$$A_2 = \omega \int \frac{Q(T)\, dT}{1 + \omega^2 T^2}.$$

The impedance of a unit area is the reciprocal of the admittance $\bar{A}$, or $Z = Z_1 + iZ_2$, where

$$Z_1 = A_1/(A_1^2 + A_2^2)$$

$$Z_2 = A_2/(A_1^2 + A_2^2).$$

For certain simple distributions of capacitance vs. time constant, it is possible to integrate the equations for A_1 and A_2 in closed form. There appears to be no experimental evidence for assigning any specific form to $Q(T)$, and we must be content at the moment to present an illustrative example arbitrarily chosen. This example does, at least, suggest qualitatively what effect a random distribution of capacitance will have on the measured impedance. Specifically, we choose as a very simple function a uniform distribution of capacitance over a range, T_1 to T_2, of time constants. Then

$$Q(T) = 1/(T_2 - T_1) \text{ for } T_1 < T < T_2$$

$$= 0 \text{ otherwise.}$$

We now have

$$A_1 = \frac{\omega^2}{T_2 - T_1} \int_{T_1}^{T_2} \frac{T\, dT}{1 + \omega^2 T^2} + \bar{G}$$

$$A_2 = \frac{\omega}{T_2 - T_1} \int_{T_1}^{T_2} \frac{dT}{1 + \omega^2 T^2}.$$

We may reduce the number of parameters by calculating $A_1/\bar{G}$ and $A_2/\bar{G}$, and by letting $K_2 = T_1/T_2$, and $K_1 = 1/[G(T_2 - T_1)]$. Then

$$A_1/\bar{G} = 1 + K_1/2 \log \frac{1 + v^2}{1 + K_2^2 v^2}$$

$$A_2/\bar{G} = K_1 \arctan \frac{(1 - K_2)v}{1 + K_2 v^2},$$

where $v = \omega T_2$.

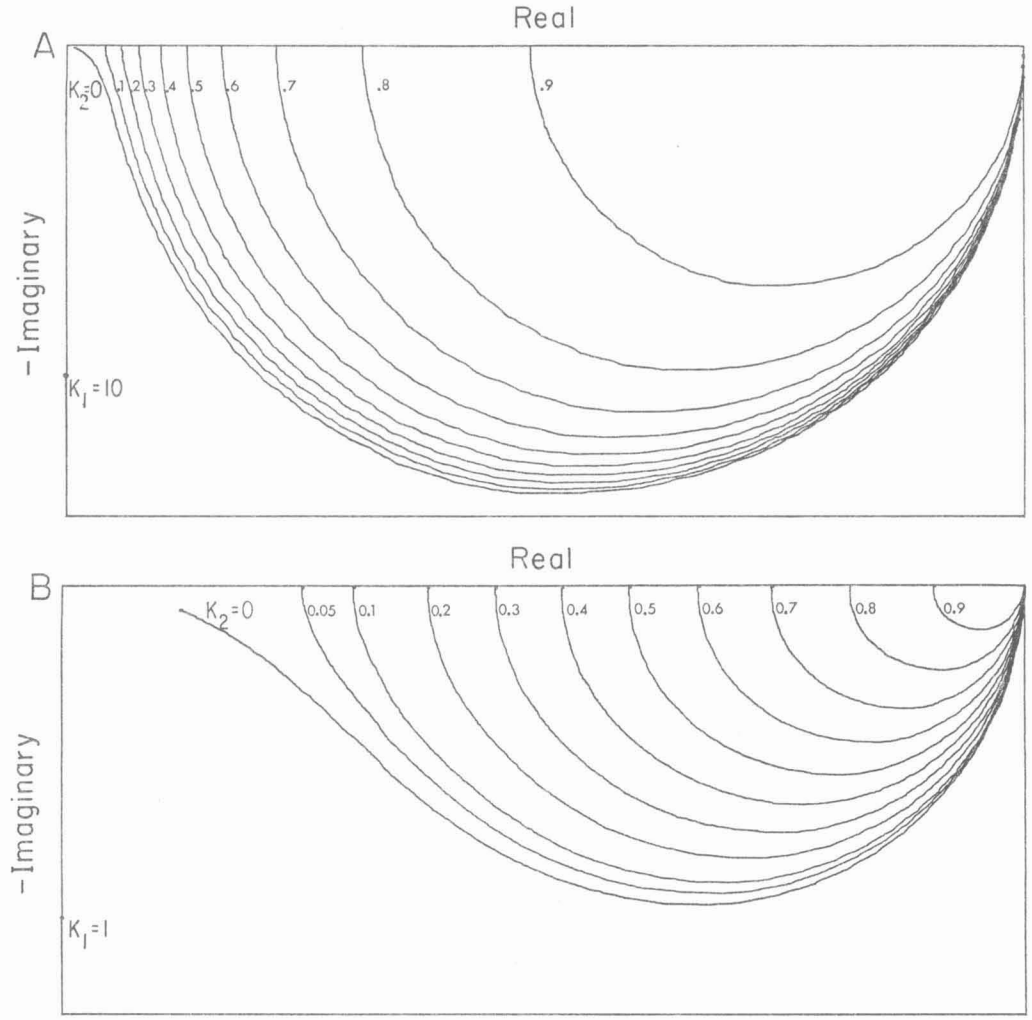

FIGURE 14 *A-E* Impedances for various statistical distributions of circuit parameters. The impedance of a statistical distribution is normalized with respect to the mean conductance, $\bar{G}$. The ratio is plotted on the complex plane for various values of $K_2 = T_1/T_2$ and of $K_1 = 1/(\bar{G}(T_2 - T_1))$ (see text). As the distribution of time constants, $T_2 - T_1$, widens, K_1 decreases from 10 to 1 to 0.05, etc., and the impedance curve flattens progressively.

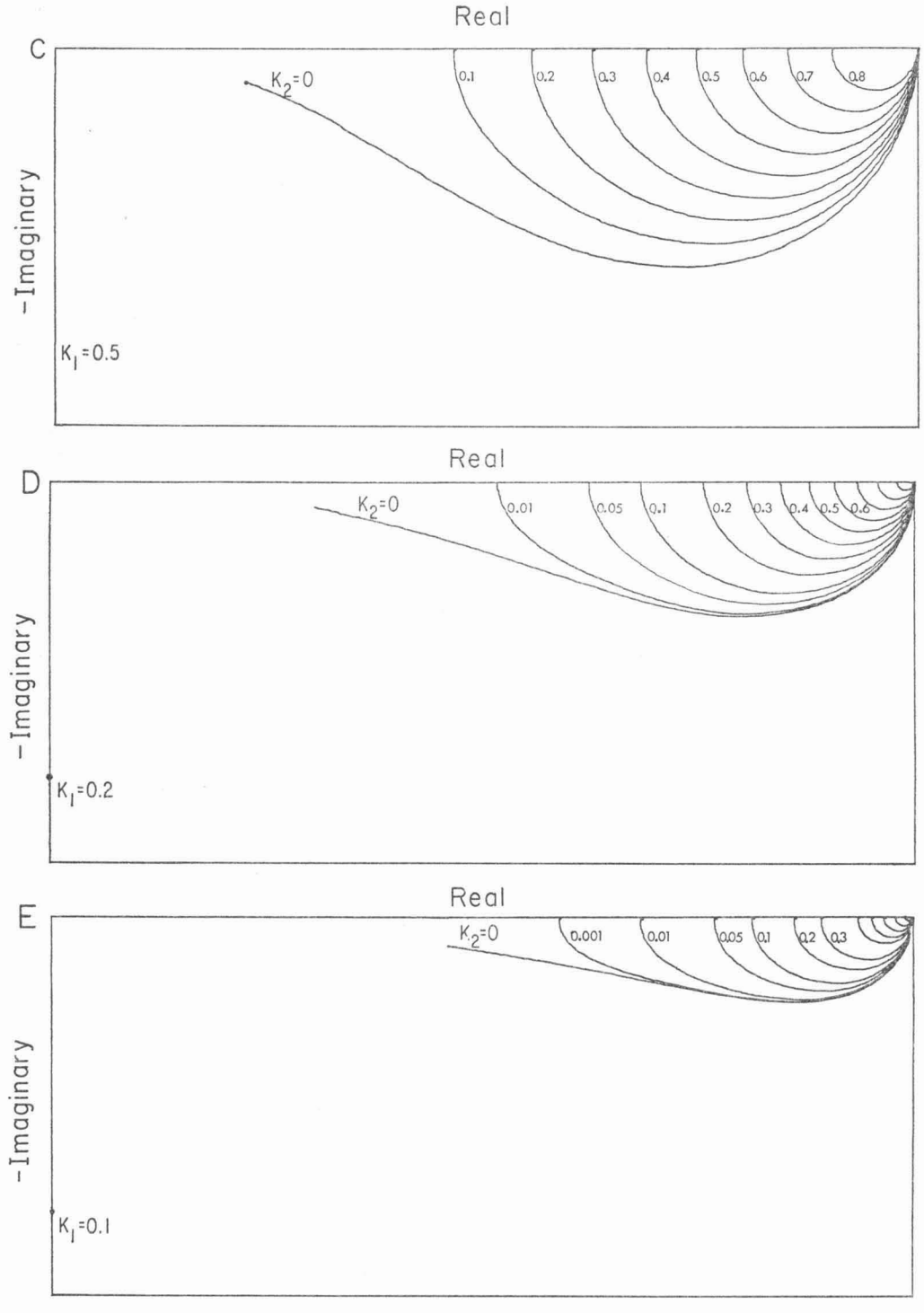
C
Real
-Imaginary
K_2=0
0.1
0.2
0.3
0.4
0.5
0.6
0.7
0.8
K_1=0.5
D
Real
-Imaginary
K_2=0
0.01
0.05
0.1
0.2
0.3
0.4
0.5
0.6
K_1=0.2
E
Real
-Imaginary
K_2=0
0.001
0.01
0.05
0.1
0.2
0.3
K_1=0.1

A computer program has been written to calculate and plot $Z\bar{G}$ derived from these functions of ν on the complex plane, for various values of K_1 and K_2 (Figs. 14 and 15). Fig. 15 shows the shapes of the complex plots for $T_1 = 0$, that is, for a uniform distribution of capacitance with time constants ranging from 0 to various values of T_2. Fig. 14 shows the effect of alterations in the band width $T_2 - T_1$.

It will be noted that many of the impedance plots depart markedly from a semicircle, and take on the flattened shape characteristic of the impedances measured in membranes and at electrode interfaces.

It is thus apparent that the characteristic flattened shape of impedances measured in cell membranes and in electrode-electrolyte interfaces do not necessarily imply either special and separate circuit elements or frequency-dependent "capacitances," but may be accounted for by statistical variation of electrical parameters from point to point over the membrane or interface.

From the foregoing discussion, we conclude that the equivalent circuit model that best describes the impedance curves obtained on the heart of the moth, is that which takes into account the processes of intercellular transmission. While an impedance, practically equivalent to that of the model proposed here, can be obtained by elaboration of the membrane model which considers the transverse tubular system, it is

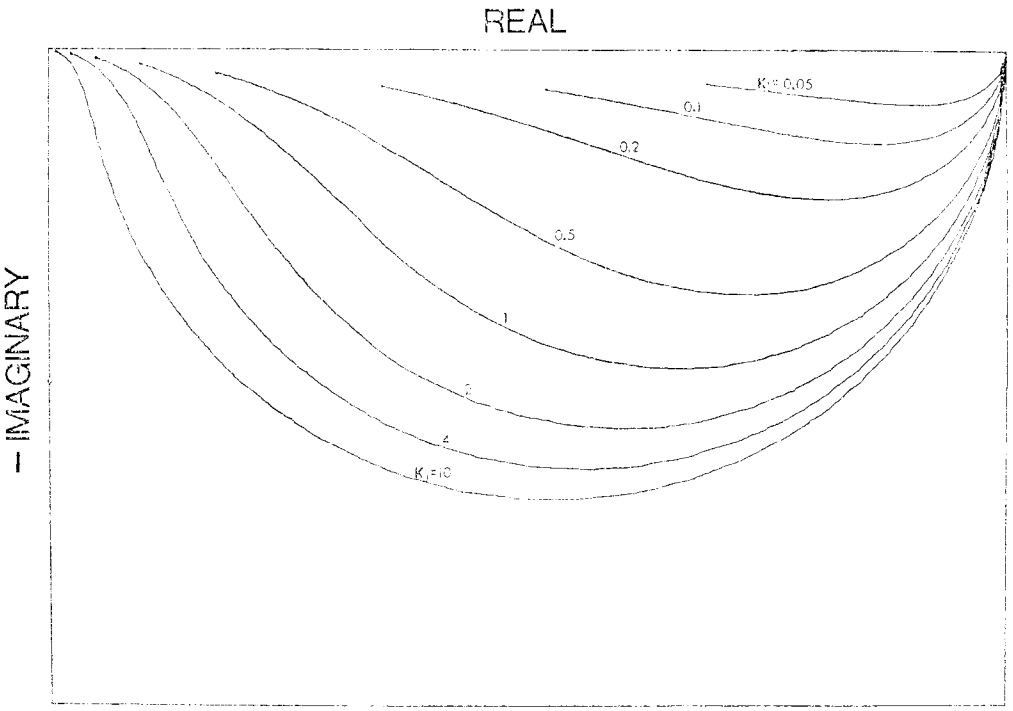

FIGURE 15 Impedances normalized as in Fig. 14 are plotted for various band widths when the time constants are distributed from 0 to T_2, so that $K_2 = 0$.

difficult to correlate the added elements with known ultrastructural components. It is our conclusion that the coupling impedance between cells is not negligible and must be considered when impedance measurements are carried out on multiple cells in a gap arrangement.

C. SIGNAL TRASMISSION BETWEEN CARDIAC CELLS

Myogenic hearts are considered functional syncytiums inasmuch as the electrical signal that precedes the contractile event appears to pass from cell to cell with little restriction. Much attention has focused on the mechanism whereby the signal crosses the intercalated disc, the boundary between cardiac cells. One group of workers believes that the junction between cardiac cells presents a formidable barrier to current spread. Measurements of electrotonic interaction between contiguous cells have been interpreted to indicate that the intercalated discs have a high electrical resistance (Tarr and Sperelakis, 1964; Kamiyama and Matsuda, 1966; Sperelakis, 1969). These workers have proposed that a chemical transmitter effects junctional transmission in the manner of other processes at cytoplasmic discontinuities such as end plates and synapses. An alternative theory suggests that the intercalated discs are specialized at restricted regions where membranes of apposed cells fuse together and Barr, 1964; Dewey, 1969; Barr, 1969). At this region, the membrane resistance is believed to be very low; therefore, current can flow from cell-to-cell to effect excitation (see review by Berger, 1972).

We would like to present as an alternative mechanism for cell-to-cell transmission, one which considers that conductance is not a prerequisite and that, in fact, a purely capacitative coupling is adequate for transmission. The model proposed here is related to the ultrastructural features of the heart of the adult moth *H. cecropia.* Electron microscopic examination of the intercalated disc region in this heart shows the presence of septate desmosomes (*SD*) and it has been proposed that the *SD* may be the functional correlates of the nexuses observed in some vertebrate hearts (McCann and Sanger, 1969). The model proposed here incorporates the values of impedance measured on the moth heart in a sucrose gap (McCann et al., 1973) and considers other structural features as presented in section A of this paper. Setting the conditions of this model such that all intercellular conductance is removed, calculation of the passive transmission of an action potential demonstrates that the capacitative coupling between cardiac cells is more than sufficient to trigger action potentials in adjunctive cells. While we do not imply, of course, that the results obtained rule out low resistance paths or other means of coupling, we simply point out that such paths are not necessary for signal transmission.

The model used here treats the cardiac tissue as an array of more or less cylindrical cells about 20 μm in diameter and 100 μm in length. These dimensions were obtained from electronmicrographs (Sanger and McCann, 1968). For simplicity it is assumed that the currents used to determine tissue impedance in the sucrose gap experiment

pass from extracellular electrolyte, through cell membranes, to the myoplasm of those cells which lie outside of the gap. These intracellular currents then flow axially in a resistive medium. The model chosen here implies that the specimen in the sucrose gap experiment presents a longitudinal impedance, Z_1, Ω/cm where Z_1 is the impedance of leaky capacitance in series with a resistor. The model further assumes an admittance of $1/Z_2$ mho/cm over that tissue surrounded by electrolyte where Z_2 is characteristic of the membrane.

The values found for these parameters by the method described in section A are (per centimeter): membrane, 0.0234 mF, 0.0178 MΩ; myoplasm, 1.489 MΩ; *SD*, 0.0149 mF, 0.289 MΩ.

As pointed out by McCann et al. (1973) the measured values are subject to large variations with time as ions leach from the cell into the sucrose or other insulating medium in the gap; however, they appear to be of the correct order of magnitude, and suffice for the present study.

On the assumption that the mean length of the cells is 100 μm, a specimen length of 1 cm contains 100 *SD* in series, and the parameter values per *SD* multiplied by the number of parallel cells are 1.49 mF and 0.00289 MΩ. Since the number of cells in parallel is not significant in the present study, we treat the specimen as composed of macrocells having the specific values given for the myoplasm and membrane, joined end to end by the capacitance 1.49 mF.

While it is possible to calculate the transfer functions for a line of the type described, to expand an action potential signal in Fourier transform, and integrate to obtain the signal form, it appears less cumbersome to solve the differential equations of the system by direct numerical analysis. The region near the junction of two cells is therefore segmented as in Fig. 16, with L the length of each segment. The membrane and myoplasm of each cell is represented by a succession of short segments (L = 20 μm), each with a series resistance $R_1 L$, a shunt capacitance $C_2 L$, and a resist-

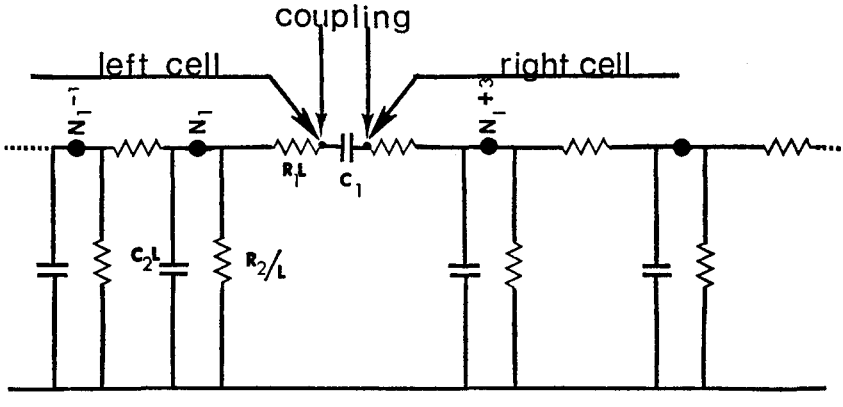

FIGURE 16 The model used in the calculation of cell to cell transmission. See text for description.

ance R_2/L. Junctions between segments are numbered 1, 2, 3, etc. Junction no. $N_1 + 1$ is the terminus of the cell on the left and no. $N_1 + 2$ that of the cell on the right. The coupling between the cells is capacitance C_1. The calculated voltage at junction no. j varies with time, and is defined as $V(j)$.

For the typical point j, let the voltage be $V(j)$. The net influx of current is zero, so that at point j, where j is not equal to $N_1 + 1$ or to $N_1 + 2$, we have

$$\frac{V(j-1) - V(j)}{R_1 L} = \frac{V(j) - V(j+1)}{R_1 L} + \frac{V(j)}{R_2} + C_2 L \frac{\mathrm{d}V(j)}{\mathrm{d}t}.$$

For a very short time interval, H, we have

$$\frac{\mathrm{d}V(j)}{\mathrm{d}t} = \frac{V(j) - W(j)}{H},$$

where $W(j)$ is the value of $V(j)$ at time t-H. These equations can be solved for $V(i)$ in the form

$$V(j) = K_1 (V(j-1) + V(j+1)) + K_2 W(j),$$

where the K's are constants.

At the junction, if I is the instantaneous value of current from N_1 to $N_1 + 3$ and Q the charge on the coupling capacitor, we have

$$\begin{aligned} Q_1 &= Q_0 + \int_{t-H}^{t} I \, \mathrm{d}t \\ &\doteq Q_0 + H(I_1 + I_0)/2, \end{aligned}$$

where subscripts 0 and 1 indicate values at t-H and t, respectively. The current, I_1 is

$$I_1 = \frac{V(N_1) - V(N_1 + 3) - Q_1/C_1}{2R_1 L}.$$

Solving these equations we have the forms

$$\begin{aligned} I_1 &= K_6 (V(N_1) - V(N_1 + 3)) - K_7 Q_0 - K_8 I_0 \\ Q_1 &= Q_0 + H(I_1 + I_0)/2 \\ V(N_1 + 1) &= V(N_1) - I_1 R_1 L \\ V(N_1 + 2) &= V(N_1 + 1) - Q_1/C_1. \end{aligned}$$

The equations for $V(j)$ can be solved, given the necessary initial conditions, for a short time interval, H. In the present problem we have chosen a segment length, $L =$

0.002 cm and a time step $H = 0.0005$ s. A computer program has been written to perform the calculations and plot the voltage, $V(j)$, as a function of distance, jL, and time, TH, where j ranges from 1 to 9 and T from 0 to 500.

The solution is calculated for an applied voltage $V(1)$, which is set equal to voltages measured in the moth heart (McCann et al. 1973). In the computer plot, distance from the junction of the cells, voltage, and time are measured on the axes shown in Fig. 17. The action potential is seen as a function of time in the left-hand boundary plane. Voltage is plotted at intervals of 0.005 s, while the corresponding functions of time at each segment are plotted at intervals of 0.002 cm.

It will be noted that in passive propagation along the left cell, the overshoot peak becomes rounded off and disappears. The signal generally decays in transmission along the cell as well as between cells. The decay along the cell is very small in the short distance shown in Fig. 17. At the junction, since we are dealing here with the capacitative coupling alone, there is a radical change in the time course of the voltage. The signal now has the appearance of a derivative of the original signal, with a maximum value roughly a third as great as the values immediately to the left of the junction, or some 22 mV. The signal on the right of the junction is seen to overshoot on its return to zero, and become slightly negative. Since the signal transmitted at the junction is primarily a derivative of the impinging signal, it would have a much greater amplitude if we had permitted the cell on the left to regenerate the action potential spike at every point. However, even with the decrement due to passive propagation in this system, a sufficient voltage is produced in the cell on the right to trigger its action potential.

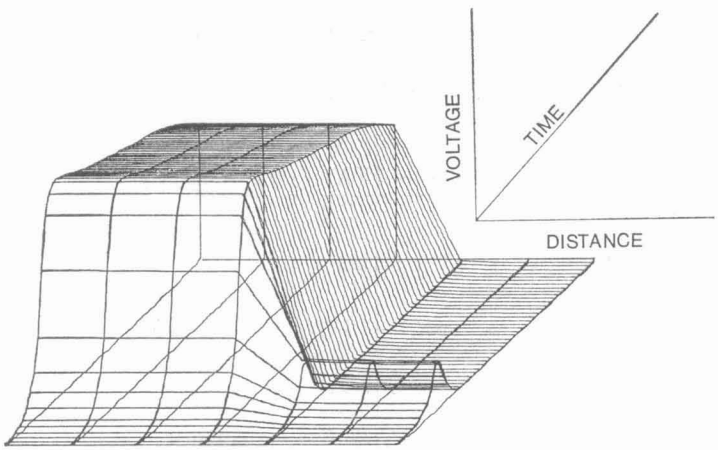

FIGURE 17 The passive spread of voltage from an action potential applied to the left cell, along that cell, across the coupling and into the right cell is calculated and plotted by a computer. The coordinate directions are indicated in the insert. Voltage is plotted at intervals of 0.005 s; corresponding functions of time, plotted at each segment at intervals of 0.002 cm.

This model incorporates a capacitative coupling between cells without specifying the anatomical correlate of this capacitance. However, it appears likely that the coupling may occur at the septate desmosomes. The presence of any conductive paths between cells would, of course, augment the transmission between cells in excess of that predicted by this model.

APPENDIX

Simulator Program

A program, EVOLVE, has been written to enable the computer to take over the tedious task of adjusting the parameter values in a simulating circuit in such a way as to match the impedance of the specimen.

An arbitrary criterion for the best fit has been chosen. It consists of the least square discrepancies between measured and calculated moduli and angles, in which weights are suitably assigned. Given the circuit configuration, then the sum of squares so weighted is a function, E, of the circuit parameters. The objective of the program, EVOLVE, is to find parameter values which minimize E.

Starting with any given parameter values, the program finds the value of E. It then selects one of the parameters at random, and applies to it a random alteration. It calculates the resulting value of E, and retains or discards the alteration according as the new E is less than or greater than the old one. Then, the cycle is repeated.

For economy of computation, the computer is instructed to form a weighted average of its ratio of successes for each variable, with weights decreasing exponentially in the past. The computer retains a "mutation range" for each variable, over which the probability of a mutation or alteration is uniformly distributed. Clearly, if the mutation range is very small, the probability of successful mutation is ½, while if the range is very large, this probability approaches zero in most instances. Hence if the success ratio approaches ½ or more, the computer is instructed to increase that range; conversely, if the success ratio falls below a given value (such as 0.35) then the range is decreased.

The number of mutations required depends, of course, upon the closeness of fit of the original estimate of parameter values, and upon the chance mutations made by the computer. To help the user in deciding when to stop the program, the computer prints the success ratio, the mutation range, the parameter value being tested, and the resulting E value, for each mutation (or at any selected period). The run is halted when the success ratios approach 0.5 and the mutation ranges are small compared with the respective parameter values, while E approaches a constant value.

The function, E, is embodied in a subprogram which solves the given circuit configuration with assigned parameter values. By appropriate specification of the subprogram, any of the configurations implied in the models described here may be optimized. Program EVOLVE has been used to determine the parameter values given in connection with each configuration shown here.

It is clear that the optima found will be local only. There is, of course, a chance that there exist other, and perhaps better, local optima, but if the program is run with large initial ranges, it is extremely likely that any separate local optima will be discovered in a series of runs.

We thank Jan Huguenin Assmus for her valuable technical assistance.

This investigation was supported in part by Public Health Service Research Grant no. HL 06132 from the National Heart and Lung Institute and a Grant-in-Aid from the American Heart Association, supported in part by the New Hampshire Heart Association, to Dr. McCann. Dr. Stibitz received support from a Public Health Service Training Grant no. HL 5322 from the NHLI.

Received for publication 13 June 1973 and in revised form 24 October 1973.

REFERENCES

BASSINGTHWAIGHTE, J. B., and H. REUTER. 1972. *In* Electrical Phenomena in the Heart. W. C. DeMello' editor. Academic Press, Inc., 353.

BARR, L. 1969. *Experientia Suppl.* **15**:102.

BERGER, W. 1972. *In* Electrical Phenomena in the Heart. W. C. DeMello, editor. Academic Press Inc., New York. 63.

COLE, K. S. 1968. Membranes, Ions and Impulses. University of California Press, Berkley.

DEWEY, M. M. and L. BARR. 1964. *J. Cell Biol.* **23**:553.

DEWEY, M. M. 1969. *Experientia Suppl.* **15**:10.

EISENBERG, R. S. 1967. *J. Gen. Physiol.* **50**:1785.

FOZZARD, H. A. 1966. *J. Physiol. (Lond).* **182**:255.

FOZZARD, H. A. 1972. *In* Electrical Phenomena in the Heart. W. C. DeMello, editor. Academic Press, Inc., New York. 219.

FREYGANG, W. H. and W. Trautwein. 1970. *J. Gen. Physiol.* **55**:524.

HEAVISIDE, O. 1887. *Electrician.* **18**:1.

KAMIYAMA, A., and K. MATSUDA. 1966. *Jap. J. Physiol.* **16**:407.

KELVIN, LORD. 1854. *Proc. Roy. Soc.* **7**:382.

MCCANN, F. V. 1965. *Ann. N. Y. Acad. Sci.* **127**:84.

MCCANN, F. V., and J. W. SANGER. 1969. *Experientia Suppl.* **15**:29.

MCCANN, F. V., G. R. STIBITZ, and J. HUGUENIN. 1973. *Biophys. J.* **13**:8.

SANGER, J. W. 1967. The ultrastructure of the moth myocardium and its adjunctive tissues. Ph.D. Thesis. Dartmouth College, Hanover, N.H.

SANGER, J. W., and F. V. MCCANN. 1968. *J. Insect. Physiol.* **14**:1105.

SPERELAKIS, N. 1969. *Experientia Suppl.* **15**:135.

STIBITZ, G. R., F.-V. MCCANN, M. BOURNE, and D. HORNIG. 1973. *J. Med. Biol. Eng.* In press.

TARR, M., and N. SPERELAKIS. 1964. *Am. J. Physiol.* **207**:691.